Available online at www.sciencedirect.com
SCIENCE DIRECT®
Journal of Power Sources 117 (2003) 7–13
JOURNAL OF POWER SOURCES
www.elsevier.com/locate/jpowsour

Energy recuperation in solid oxide fuel cell (SOFC) and gas turbine (GT) combined system

Prapan Kuchonthara[a], Sankar Bhattacharya[b], Atsushi Tsutsumi[a,*]

[a]*Department of Chemical System Engineering, The University of Tokyo, 7-3-1 Hongo, Bunkyo-ku, Tokyo 113-8656, Japan*
[b]*Cooperative Research Centre for Clean Power from Lignite, 8/677 Springvale Road, Mulgrave, Vic. 3170, Australia*

Received 22 July 2002; accepted 29 December 2002

Abstract

A combined power generation system consisting of a solid oxide fuel cell (SOFC) and a gas turbine (GT) with steam and heat recuperation (HR) was evaluated using a commercial process simulation tool, ASPEN Plus. The effect of steam recuperation (SR) on the overall efficiency of the combined system was investigated by comparing the SOFC–GT during heat and steam recuperation (HSR) against the system during only heat recuperation. At low turbine inlet temperatures (TITs), the overall efficiency of the SOFC–GT combined system with heat and steam recuperation improved by showing an increase in TIT and a reduction in pressure ratio (PR). On the other hand, at high TITs, the opposite trend was observed. The integration of steam recuperation was found to improve the overall efficiency and specific power of SOFC–GT combined systems with a relatively compact SOFC component.
© 2003 Elsevier Science B.V. All rights reserved.

Keywords: Solid oxide fuel cell; Gas turbine; Combination; Energy recuperation

1. Introduction

Fuel cells are promising power generation systems of high efficiency because they can convert the free energy change of a chemical reaction directly into electrical energy. Among different kinds of fuel cells, a solid oxide fuel cell (SOFC) that is operated at high temperature has been particularly interesting because it is effluent, at about 1173 K, is suitable for integration with gas turbine (GT) cycles. In this scheme, the thermal energy generated by electrochemical reactions in the fuel cell is utilized to produce more power output by a GT cycle. As the result, higher overall efficiency is expected in comparison with that obtained from individual systems.

Recently, several articles have been devoted to the study of SOFC–GT combined power generation systems [1–5]. Most of these studies have reported a natural gas-fueled SOFC–GT system with steam reforming and heat recuperation (HR, air preheating). Palsson et al. [1] developed a two-dimensional, steady-state SOFC model and proposed a combined system featuring external pre-reforming and recirculation of anode gases. They reported that the maximum efficiency of 65% (LHV) was obtained at a pressure ratio of 2. Increasing the turbine inlet temperature (TIT) does not lead to an improvement of efficiency or specific power because at higher TIT, more fuel is being consumed in the gas turbine, decreasing the fuel flow to the SOFC unit. Tanaka et al. [3] have designed and evaluated a SOFC–GT combined system based on system performance and cost/energy pay-back times. They mentioned the similar result for the influence of TIT on overall efficiency. A small GT power output to net output is desirable for overall performance. In fact, the GT output from a combined SOFC–GT system is about one-third of the total output [1]. Thus, in commercial power generation systems, large SOFC systems with the capacity of several tens of MW are required to compete with conventional power plants. However, the capacity of current SOFC technology is on a level of sub MW to several MW.

Since the efficiency of GT is considerably lower than that of SOFC in such a combined system, an improvement to GT efficiency by means of advanced cycle integration technologies could increase the overall efficiency. Moreover, it contributes to a possibility of a reduction in size required for a commercial scale SOFC power plant by virtue of lowering the fuel utilization fraction of the SOFC. In general, an improvement of GT performance was obtained by recovering heat in the turbine exhaust. The heat can be used to preheat compressed air stream, to generate steam for a

* Corresponding author. Tel.: +81-3-5841-7336; fax: +81-3-5841-7270.
E-mail address: tsutsumi@chemsys.t.u-tokyo.ac.jp (A. Tsutsumi).

0378-7753/03/$ – see front matter © 2003 Elsevier Science B.V. All rights reserved.
doi:10.1016/S0378-7753(03)00009-0

Nomenclature

A	coefficient in Eq. (5) (V)
B	coefficient in Eq. (5) (V)
CA	cell area (m^2)
E	cell voltage (V)
F	Faraday constant (=96,487) (C mol^{-1})
i	current density (A m^{-2})
i_0	exchange current density (A m^{-2})
i_L	limiting current density (A m^{-2})
K_T	equilibrium constant
LHV	lower heating value of fuel (J kg^{-1})
m	mass flow rate (kg s^{-1})
n	molar flow rate (mol s^{-1})
n_e	number of electrons
p	partial pressure (Pa)
p_0	reference pressure (Pa)
P_c	power density (J s^{-1} m^{-2})
P_{FC}	power generated by fuel cell (J s^{-1})
$Q_{GT,in}$	heat supplied to gas turbine cycle (J s^{-1})
Q_{out}	heat generated by fuel cell (J s^{-1})
Q_{rec}	energy recuperation rate
R	gas constant (=8.314) (J mol^{-1} K^{-1})
R_e	area-specific ohmic resistance (Ω m^2)
T	temperature (K)
TIT	turbine inlet temperature (K)
U_a	air (oxygen) utilization factor
U_f	fuel utilization factor
V_o	polarization (V)
w	specific power (J kg^{-1})
w_{FC}	power rate of fuel cell
w_{GT}	power rate of gas turbine

Greek letters

η_{th}	overall system efficiency, LHV basis
η_{FC}	power generation efficiency of SOFC, LHV basis
η_{GT}	power generation efficiency of GT, LHV basis

Subscripts

act	activity
air	air
conc	concentration
f	fuel
in	inlet
ohm	ohmic
ox	oxygen
r	reversible

Superscripts

in	inlet
I	inlet condition

bottoming steam turbine (ST) cycle, and to directly injecting to the GT combustor. Those configurations were contributed in a recuperative GT cycle (RGT), gas turbine combined cycle (GTCC), and a steam-injected gas turbine (STIG) cycle. Several studies have been devoted to study on such enhanced GT systems for achieving higher system efficiency [6–10].

According to the previous studies on SOFC–GT combined systems, the heat from GT exhaust is usually recuperated for air preheating (heat recuperation) in a recuperator, like the recuperative GT cycle. However, there are no studies on such a combined system engaging other enhanced GT cycle. In this paper, another energy recuperation technology, steam recuperation (SR), was employed to recover more heat from the GT exhaust as the aim to increase the overall efficiency and specific power. The superheated steam generated from the heat of the GT exhaust is injected into the GT combustion chamber. The system configuration is somewhat similar to the STIG incorporated with air preheating process. This leads to greater power output from the GT due to an increase in the mass flow of steam the process of expansion. By using a process simulation tool, ASPEN Plus, a conceptual design of a SOFC–GT combined system with heat and steam recuperation (HSR) was preformed so as to improve system performance.

2. SOFC model

Electrochemical oxidation reactions of H_2 in the SOFC proceed as follows [11,12]:

$$H_2 + O^{2-} \rightarrow H_2O + 2e^- \quad \text{(anode)}$$

$$\tfrac{1}{2}\,O_2 + 2e^- \rightarrow O^{2-} \quad \text{(cathode)}$$

$$H_2 + \tfrac{1}{2}\,O_2 \rightarrow H_2O \quad \text{(overall)} \tag{1}$$

The theoretical open circuit cell voltage (E_r) can be determined by the Nernst equation:

$$E_r = \frac{RT}{2F}\ln K_T - \frac{RT}{4F}\ln\left(\frac{(p^I_{H_2O})^2 p_0}{(p^I_{H_2})^2 p^I_{O_2}}\right) \tag{2}$$

where T denotes the operating cell temperature; and K_T the equilibrium constant of the overall reaction at the temperature considered. The first term on the right hand side of Eq. (2) shows the effect of the temperature on the cell voltage while the second term shows the effect of the pressures of reactants and product on cell voltage. In a practical fuel cell, the operating cell voltage (E) is less than the reversible cell potential (E_r). The drop in cell voltage is attributed by the irreversibility, so-called overpotential or polarization. The polarization losses can be distinguished into three types; ohmic polarization ($V_{o,ohm}$), activation polarization ($V_{o,act}$), and concentration polarization ($V_{o,conc}$). The magnitude of these polarizations increases alongside the increase in current density, thus reducing cell voltage and voltage efficiency. The cell voltage can be estimated as follows [13]:

$$E(i) = E_r - V_{o,ohm} - V_{o,act} - V_{o,conc} \tag{3}$$

wherein

$$V_{o,ohm} = iR_e \tag{4}$$

$$V_{o,act} = A \ln\left(\frac{i}{i_0}\right) \tag{5}$$

$$V_{o,conc} = -B \ln\left(1 - \frac{i}{i_L}\right) \tag{6}$$

It should be noted here that in case of fuel cell operating at high temperature level, like SOFC, the polarization loss is dominantly derived from the ohmic polarization [3].

The activation and concentration polarizations can be derived from the Tafel equation. Other parameters in the SOFC model calculation, air utilization factor (U_a), fuel utilization factor (U_f), power density (P_c), and power generated by SOFC (P_{FC}) are listed as follows:

$$U_a = \frac{n_{ox}^{in} - n_{ox}^{out}}{n_{ox}^{in}} \tag{7}$$

$$U_f = \frac{n_f^{in} - n_f^{out}}{n_f^{in}} \tag{8}$$

$$P_c = iE = \frac{U_f n_f^{in} n_e F}{CA} E \tag{9}$$

$$P_{FC} = U_f n_f^{in} n_e FE = P_c CA \tag{10}$$

wherein, n_{ox} and n_f denote the mole flow of oxygen and fuel; CA the cell area; and n_e the number of electrons (two for hydrogen). The heat generated by irreversibility at the electrodes in the SOFC (Q_{out}) is expressed by:

$$Q_{out} = U_f m_f LHV_f - P_{FC} \tag{11}$$

m_f and LHV_f denote the mass flow and lower heating value of the fuel, respectively. It is assumed that the heat is recovered in the SOFC block by exchanging with the fuel and air streams. The outlet stream temperature of the SOFC can be determined by the thermal balance across the whole cell.

3. Combined system configuration and methodology

The SOFC calculations described here were performed using Fortran calculation modules in ASPEN Plus, whereas other components constituting the system are modeled as standard unit operation models. Schematic configurations of the combined system are illustrated in Fig. 1a and b for a SOFC–GT with heat recuperation system and a SOFC–GT with heat and steam recuperation system, respectively. The SOFC–GT combined system mainly consists of a SOFC module and a GT cycle connected together in series, in which the SOFC module was integrated as a topping cycle. Both air and fuel are compressed and introduced into the SOFC. The SOFC produces both heat and electricity through the electrochemical reactions of fuel. The temperature in the

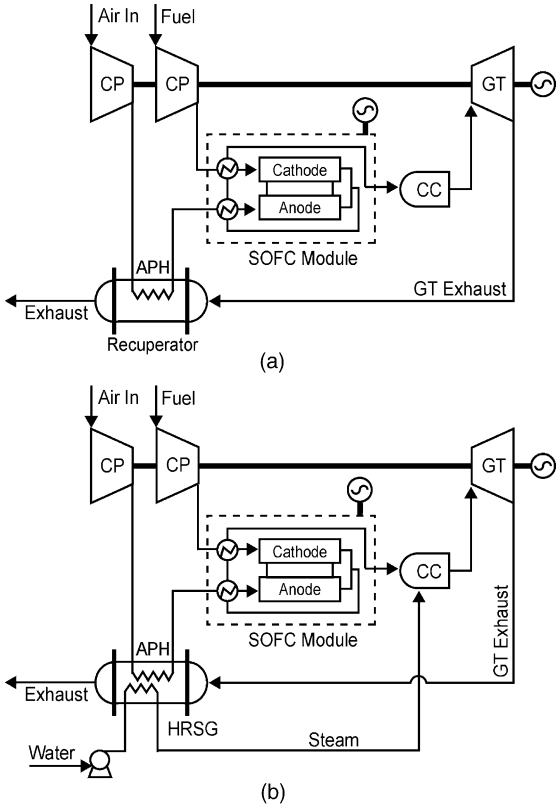

Fig. 1. Schematic diagrams of SOFC–GT combined systems: (a) SOFC–GT with HR and (b) SOFC–GT with HSR.

SOFC is kept constant (~1273 K) by utilizing the heat produced in the SOFC itself for preheating both the air and fuel streams. Remaining (unreacted) fuel from the SOFC is burnt with depleted air in a GT combustor. The hot combustion gases are expanded in the GT to produce power. Energy recuperation is employed in the system to recover heat from the GT exhaust in two different configurations. The SOFC–GT with HR employed an air preheating system for recuperating heat from the GT exhaust. In addition to the air preheator, a heat recovery steam generator (HRSG) was installed on the system in the case of the SOFC–GT with HSR. In this case, the heat from the GT exhaust is not only used for preheating compressed air stream but also for generating steam in the HRSG. The generated steam is directly injected into the GT combustor as recuperated steam, leading to an increase in GT power output owing to a rise in net mass flow through the process of expansion.

The systems mentioned were simulated and evaluated with the following hypotheses: (a) hydrogen (H_2) was used as fuel; (b) working pressure ratios (PR) of 5, 7, 10, and 15 were considered; (c) thermodynamic properties based on Peng–Robinson equation of state with the Boston–Mathias alpha function, which is appropriate for power generation process, were used; (d) thermodynamic properties of gases, liquid water and steam were taken from databases available in ASPEN Plus; (e) a polytropic efficiency of 0.9 for both the

Table 1
Assumptions and input parameters in system evaluation

Solid oxide fuel cell (SOFC)	
dc–ac converter efficiency	0.95
Fuel utilization factor, U_f	0.50–0.95
Air utilization factor, U_a	0.30
Cell operating temperature (K)	1273
Area-specific resistance ($\Omega\,cm^2$)	0.5
Current density (mA cm^{-2})	400
Exchange current density (mA cm^{-2})	300
Limiting current density (mA cm^{-2})	900
Constant A parameter (Eq. (5)) (V)	0.03
Constant B parameter (Eq. (6)) (V)	0.08
Gas turbine cycle	
Pressure ratio	5, 7, 10, 15
Polytropic efficiency	0.9
Mechanical efficiency (compression and expansion)	0.98
Minimum stack temperature (K)	423
Recuperator efficiency	0.80
Pressure drop	
SOFC cell (%)	3
Combustor (%)	2
Heat exchanger (each) (%)	2

compression and expansion processes was given; (f) no additional turbine blade cooling was considered; (g) a pressure loss of 2–3% was allotted to heat exchangers, SOFC stacks, the HRSG, and the GT combustion chamber; (h) the recuperator efficiency of 0.80 was employed for estimating hot air temperature; (i) the steam temperature was assumed to be either the same as the hot air temperature or not exceeding the steam temperature limit, 823 K in this work; (j) current density and cell operating temperature in the SOFC were set as certain values for all system analyses; (k) the minimum temperature of the exhaust gas from the HRSG was 423 K, which was higher than the corresponding dew point temperature in order to prevent condensation problems. Basic assumptions and input parameters of the system simulation are summarized in Table 1.

The evaluations were carried out by varying fuel utilization factor (U_f) in the range of 0.50–0.95 at a constant air utilization factor (U_a) of 0.30. Here, as expressed in Eqs. (7) and (8), the U_a and U_f factors are ratios of oxygen and fuel consumed in the SOFC to the total oxygen and fuel supplied to the system, respectively, indicating the amount of oxygen in air and fuel remaining after the electrochemical reactions in the SOFC. Lower value of the U_f factor means a greater portion of the fuel is combusted with depleted air from the SOFC in the GT combustor. This leads to a higher turbine inlet temperature. On the other hand, lower TIT is a result of a higher U_f factor, owing to less remaining fuel. It was confirmed that the remaining amount of oxygen in air is enough for combustion in the GT combustor as long as the U_f value is larger than the U_a value.

According to the energy flow diagrams of the two SOFC–GT combined systems, as shown in Fig. 2a and b, energy recuperation rate (Q_{rec}) and power rate of the SOFC (w_{FC}),

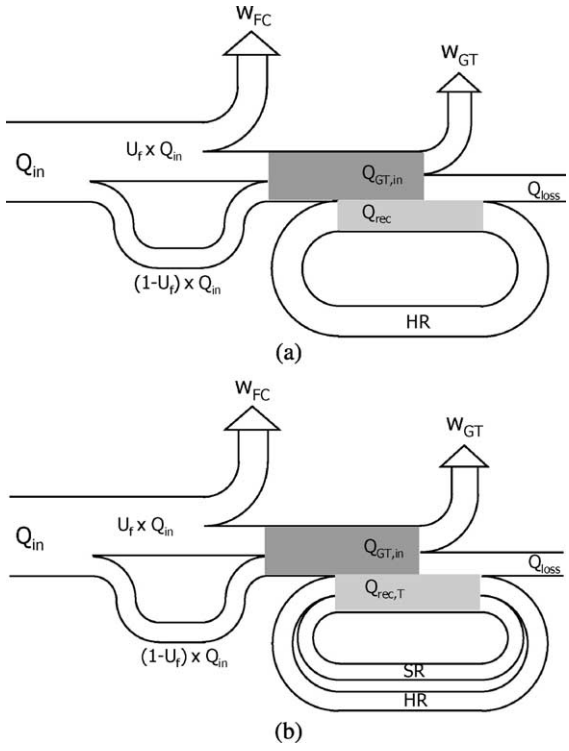

Fig. 2. Energy flow diagrams of SOFC–GT combined systems: (a) SOFC–GT with HR and (b) SOFC–GT with HSR.

and power rate of the GT (w_{GT}) can be determined based on the energy input to the system (heating value of fuel). The comparison of the two systems was conducted at a given operating PR to evaluate the contribution of steam recuperation to system improvement. In addition, the combined systems with different operating TIT and PR were assessed and discussed.

4. Results and discussion

4.1. Effects of steam recuperation (SR) on system performance

Energy recuperation rate (Q_{rec}) and power rate of the SOFC (w_{FC}) as well as the power rate of the GT (w_{GT}) in the SOFC–GT combined system with HR and HSR at a PR of 5 were plotted against U_f in Fig. 3. Fig. 4 shows the relationship between TIT and U_f as well as the relationship between overall efficiency (η_{th}) and U_f of the two systems, for the same PR of 5. Here, η_{th} denotes the summation of w_{FC} and w_{GT}. In the case of the SOFC–GT with HSR, two different configurations for steam temperature were taken into consideration and assessed. First, the steam temperature was set to be close to the preheated air temperature after the recuperator. Second, the steam temperature was limited to 823 K. It was considered that in some cases the temperature of preheated air is too high to practically generate the steam at such high temperature. The maximum steam temperature

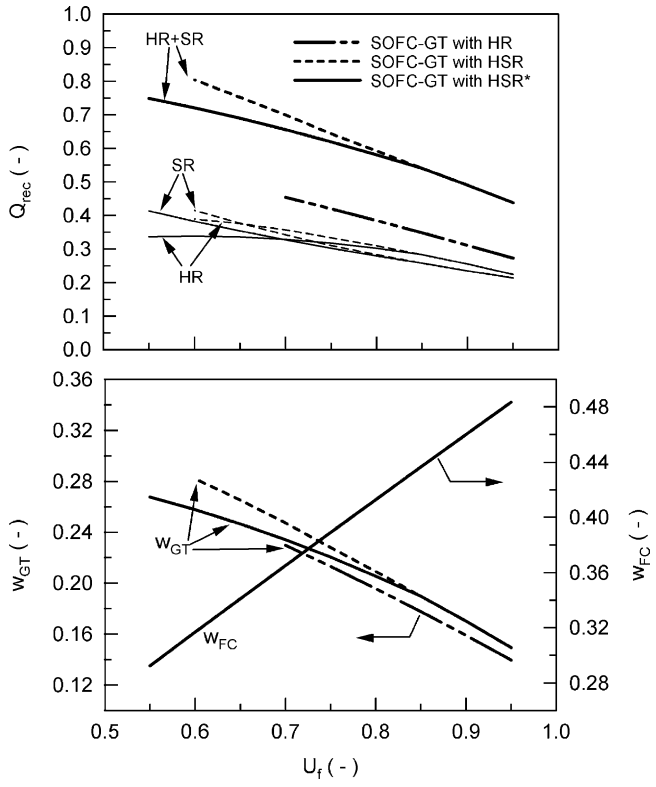

Fig. 3. Energy recuperation rate (Q_{rec}) and power rate of SOFC (w_{FC}), and power rate of GT (w_{GT}) in combined systems as a function of U_f ($PR = 5$). (*) With limitation of $T_{steam,max} = 823$ K.

should be considered, corresponding to the steam boiler technologies.

As can be seen in Fig. 3, the system with HSR has a higher Q_{rec} than that with HR, indicating a larger w_{GT} and same w_{FC}. Furthermore, the SOFC–GT with HSR produced a higher η_{th} value than the system with HR at a given U_f, as can be seen in Fig. 4. It can be concluded that in addition to heat recuperation, steam recuperation can increase energy recuperation rate, Q_{rec}, resulting in the increase in w_{GT} and

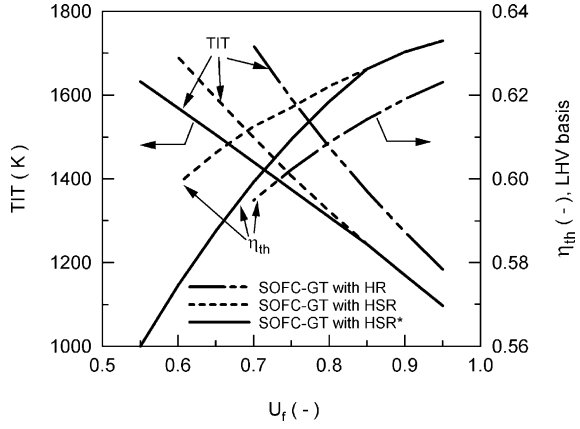

Fig. 4. Turbine inlet temperature (TIT) and overall efficiency (η_{th}) of combined systems as a function of U_f ($PR = 5$). (*) With limitation of $T_{steam,max} = 823$ K.

η_{th}. However, it was seen from Fig. 3 that the increment in w_{GT} is less than that in Q_{rec} for the given U_f. This is due to the reduction in TIT caused by steam recuperation. Since steam has a higher specific heat capacity than air, steam recuperation increases Q_{rec} and GT efficiency, but reduces TIT at the given U_f.

In general, steam temperature has a maximum limit in an operation depending on specifications of the steam generator (boiler). In this case, the maximum steam temperature ($T_{steam,max}$) in the SOFC–GT with HSR is assumed to be 823 K. With decreasing U_f, the steam temperature increases because both TIT and GT outlet temperature increase. At $U_f = 0.85$, the steam temperature was found to reach $T_{steam,max}$ (=823 K). When the U_f is lower than 0.85, the steam temperature in the system with the limitation was kept at 823 K, which was lower than the temperature of the preheated air. The lower steam temperature reduces TIT as well as Q_{rec}, leading to a decrease in η_{th} in comparison with the system without the steam temperature limitation, as can been seen in Figs. 3 and 4. Despite the adverse effect of the limitation of steam temperature, the η_{th} of the SOFC–GT with HSR is still higher than that of the system with HR. It can be, therefore, concluded that steam recuperation with a limitation in steam temperature can also improve the overall efficiency as well as the power output by virtue of the increase in energy provided for the GT.

Fig. 5 shows the effect of U_f on energy recuperation rate (Q_{rec}) and power rates (w_{GT}, w_{FC}) in the SOFC–GT combined systems at a PR of 10. Turbine inlet temperature and

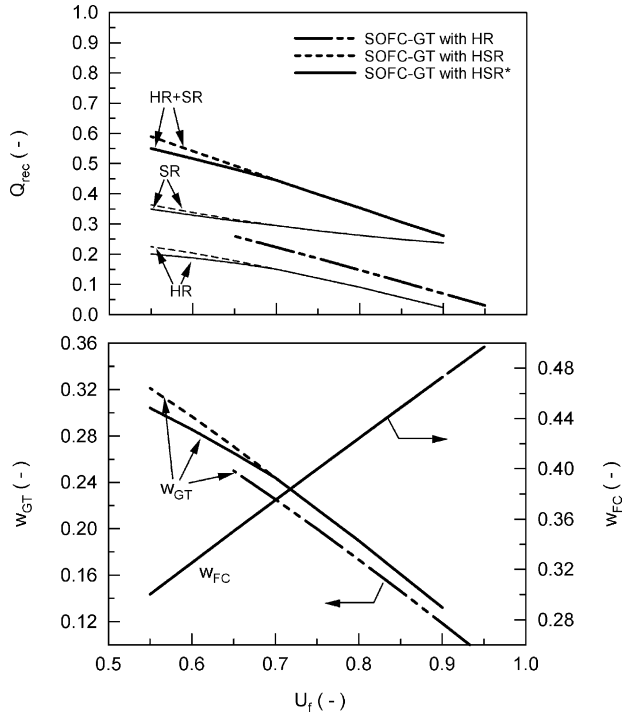

Fig. 5. Energy recuperation rate (Q_{rec}) and power rate of SOFC (w_{FC}), and power rate of GT (w_{GT}) in combined systems as a function of U_f ($PR = 10$). (*) With limitation of $T_{steam,max} = 823$ K.

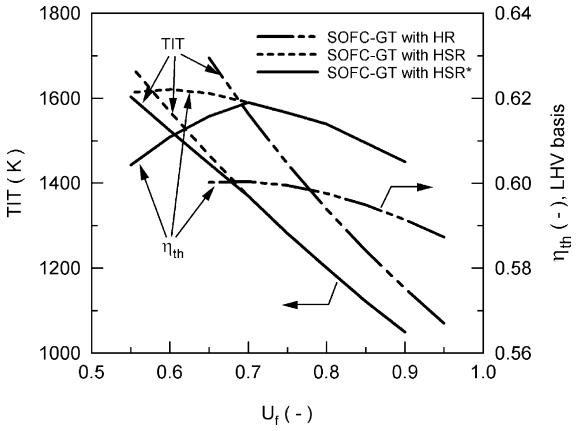

Fig. 6. TIT and overall efficiency (η_{th}) of combined systems as a function of U_f ($PR = 10$). (*) With limitation of $T_{steam,max} = 823$ K.

overall efficiency (η_{th}) were plotted against U_f in Fig. 6. It is clear that Q_{rec} as well as w_{GT} in the system with HSR are larger compared to the system with HR. This leads to an increase in η_{th}, as shown in Fig. 6. Comparing with PR = 5 (see Fig. 4), it was found that the synergetic effect of steam recuperation becomes more significant at higher PRs.

4.2. Effects of turbine inlet temperature and pressure ratio on system performance

The overall efficiency (η_{th}) and specific power (w) of the SOFC–GT with HSR ($T_{steam,max} = 823$ K) were plotted against TIT with a variation of pressure ratios, in Fig. 7. Here, the specific work is defined as the total power output divided by the mass flow rate of air. The η_{th} versus TIT curve

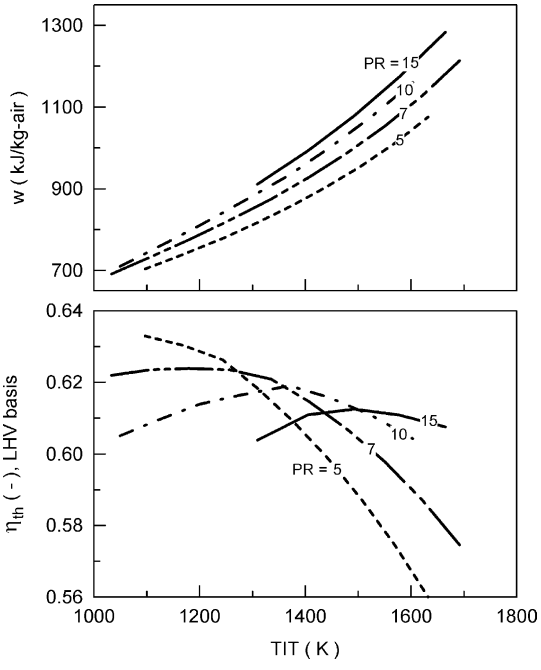

Fig. 7. Influences of TIT and PR on overall efficiency (η_{th}) and specific power (w) in SOFC–GT with HSR ($T_{steam,max} = 823$ K).

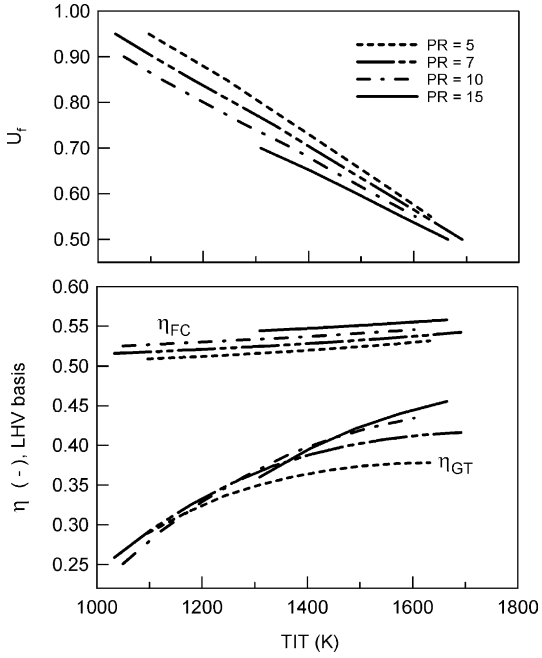

Fig. 8. Influences of TIT and PR on U_f, SOFC efficiency (η_{FC}), and GT efficiency (η_{GT}) in SOFC–GT with HSR ($T_{steam,max} = 823$ K).

appears to exhibit a peak for the given PR. It was observed that the specific power monotonously increase with the increase in TIT for all PRs.

Fig. 8 illustrates the influences of TIT on U_f, the power generation efficiency of the SOFC (η_{FC}), and the power generation efficiency of the GT (η_{GT}) in the combined system. Here, η_{FC} and η_{GT} denote ratios of power output to the energy input of each system, SOFC and GT, respectively (see Fig. 2), which are defined by

$$\eta_{FC} = \frac{w_{FC}}{U_f} \tag{12}$$

$$\eta_{GT} = \frac{w_{GT}}{Q_{GT,in}} = \frac{w_{GT}}{(1 - w_{FC})} \tag{13}$$

wherein, w_{FC} and w_{GT} denote power rate of the SOFC and the GT, respectively, based on total energy input to the system (Q_{in}), which is equivalent to the lower heating value of the fuel; and $Q_{GT,in}$ represents the energy input to the GT. The lower U_f leads to more fuel utilization in GT, resulting in higher TIT. Although the increase in TIT reduces the ratio of the amount of fuel consumed in the SOFC (lower U_f), as shown in Fig. 8, the increase in TIT increases the η_{GT}. Hence, the overall efficiency (η_{th}) decreases with the increase in TIT because η_{FC} is considerably higher than η_{GT}. This gives a good account of the tendency of η_{th} to decrease with the increase in TIT at high TITs. On the other hand, at low TITs η_{GT} declines significantly (see Fig. 8). This reduces η_{th} despite the large U_f. It can be, therefore, considered that, with increasing TIT, the overall efficiency increases to a maximum and subsequently decreases.

At low TITs, η_{th} was found to decrease with the increase in PR, while the opposite trend was observed at high TITs.

An increase in PR reduces GT outlet temperature as well as Q_{rec}, requiring more fuel consumption in the GT combustor to attain the same TIT. This means that the increase in PR reduces U_f. Therefore, a higher PR gives lower η_{th} at low TITs, as can be seen in Fig. 7. On the other hand, at high TITs, η_{GT} was found to improve significantly with increasing PR. This is attributed to larger power generation in the GT expansion process at higher PR. In addition, the adverse effect of PR on U_f becomes insignificant at high TITs. Therefore, the improvement of η_{GT} at higher PR overcomes the adverse effect of PR. This leads to the improvement of η_{th} at high TITs.

In Fig. 7, the optimum point of η_{th} was observed to shift to higher TIT as PR increased. It is noteworthy that in spite of the somewhat lower η_{th} of the high PR systems at the optimum point, a significant increase in specific power was observed. The increase in TIT (lower in U_f) means the fuel is consumed in the GT combustor rather than in the SOFC. This indicates the higher power fraction of GT to the overall SOFC–GT system, represented by the increase in power rate of GT as can be seen in Figs. 3 and 5. This result suggests that the SOFC–GT with HSR operated at high PR can reduce the power size of the SOFC with keeping the overall efficiency relatively high. This contributes to diminish the cost problem of the fuel cell in a combined system of large overall power output.

5. Conclusions

The integration of steam recuperation into a SOFC–GT combined system with heat recuperation was evaluated by using a process simulation tool, ASPEN Plus. It was found that the system with heat and steam recuperation gave higher overall efficiency than the system with only heat recuperation. The integration of steam recuperation increases the energy recuperation rate from the waste heat in the GT exhaust, leading to the improvement in GT efficiency. The synergetic effect of steam recuperation became more significant at higher PRs. The limitation on steam temperature generated in the heat recovery steam boiler obviously diminishes the synergetic effect due to the drop in the energy recuperation rate and the turbine inlet temperature. In addition, at low TITs, the increase in TIT was found to increase the overall efficiency by means of the improvement in GT efficiency. On the contrary, at high TITs, the overall efficiency decreased with the increase in TIT because of a lower U_f. Thus, the overall efficiency increases to a maximum and subsequently decreases as TIT increases. With an increasing PR, the overall efficiency decreases at low TITs, whereas at high TITs, the improvement in GT efficiency induced by the increase in PR overcomes the adverse effect of PR on the energy recuperation, resulting in an increase in overall efficiency with PR. In addition, the specific power was found to gradually increases as both TIT and PR increase. Hence, high power output with high efficiency can achieve in the system operating at high TIT with an optimal PR. This finding suggests that the size of the SOFC is likely reduced with an appropriate operating condition and integration of heat and steam recuperation, while both the overall efficiency and specific power are considerably high.

Acknowledgements

The authors would like to thank Core Research for Evolutional Science and Technology (CREST) of Japan for their financial support, and the Cooperative Research Centre for Clean Power from Lignite, Australia, for their collaboration.

References

[1] J. Palsson, A. Selimovic, L. Sjunnesson, J. Power Sources 86 (2000) 442–448.
[2] A. Khandkar, J. Hartvigsen, S. Elangovan, Solid State Ionics 135 (2000) 325–330.
[3] K. Tanaka, C. Wen, K. Yamada, Fuel 79 (2000) 1493–1507.
[4] E. Riensche, E. Achenbach, D. Froning, M.R. Haines, W.K. Heidug, A. Lokurlu, S. von Andrian, J. Power Sources 86 (2000) 404–410.
[5] P. Costamagna, L. Magistri, A.F. Massardo, J. Power Sources 96 (2001) 352–368.
[6] K.F. Kesser, M.A. Hoffman, J.W. Baughn, Trans. ASME J. Eng. Gas Turbines Power 116 (1994) 277–284.
[7] M. De Paepe, E. Dick, Int. J. Energy Res. 24 (2000) 1081–1107.
[8] W.L.R. Gallo, Energy Conserv. Manage. 38 (1997) 1595–1604.
[9] O. Bolland, J.F. Stadaas, ASME Paper, No. 93-GT-57, 1993.
[10] E. Macchi, S. Consonni, G. Lozza, P. Chiesa, Trans. ASME J. Eng. Gas Turbines Power 117 (1995) 489–498.
[11] J.O'M. Bockris, S. Srinivasan, Fuel Cells: Their Electrochemistry, McGraw-Hill, New York, 1969.
[12] C. Berger, Handbook of Fuel Cell Technology, Prentice-Hall, New York, 1968.
[13] J. Larminie, A. Dicks, Fuel Cell Systems Explained, Wiley, London, 2000.